

Recovery of Compactly Supported Functions from Spectrogram Measurements via Lifting

Mark Iwen

markiwen@math.msu.edu

MICHIGAN STATE
U N I V E R S I T Y

2017

Friday, July 7th, 2017

Joint work with...



Sami Merhi (Michigan State University)

Joint work with...



Aditya Viswanathan (University of Michigan - Dearborn)

Motivation

Applications: The phase-retrieval problem arises whenever the detectors can only capture *intensity* measurements. For example,

- X-ray crystallography
- Diffraction imaging
- Ptychographic Imaging
- ...

Our goals: Approaching realistic measurement designs compatible with, e.g., ptychography, coupled with computationally efficient and robust recovery algorithms.

Motivation

Applications: The phase-retrieval problem arises whenever the detectors can only capture *intensity* measurements. For example,

- X-ray crystallography
- Diffraction imaging
- Ptychographic Imaging
- ...

Our goals: Approaching realistic measurement designs compatible with, e.g., ptychography, coupled with computationally efficient and robust recovery algorithms.

Motivating Application

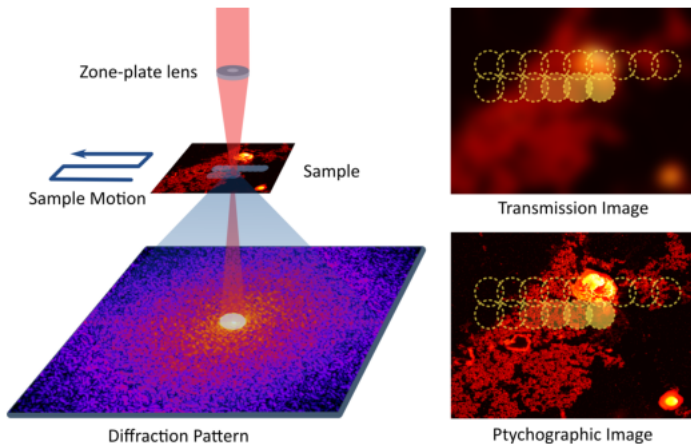


Figure: Ptychographic Imaging

Algorithms for Discrete Phase Retrieval

- There has been a good deal of work on signal recovery from phaseless STFT measurements in the *discrete setting*:
 - ▶ First f and g are modeled as vectors ab initio,
 - ▶ Then recovered from discrete STFT magnitude measurements.
- Recovery techniques include
 - ▶ Iterative methods (Alt. Proj. for STFT) along the lines of Griffin and Lim [8, 12],
 - ▶ Alternating Projections [7],
 - ▶ Graph theoretic methods for Gabor frames based on polarization [11, 9],
 - ▶ Semidefinite relaxation-based methods [5], and others [2, 1, 4, 3].

Signal Recovery from STFT Measurements

- In 1-D ptychography [10, 7], a compactly supported specimen $f : \mathbb{R} \rightarrow \mathbb{C}$, is scanned by a focused beam $g : \mathbb{R} \rightarrow \mathbb{C}$ which translates across the specimen in fixed overlapping shifts $l_1, \dots, l_K \in \mathbb{R}$.
- At each such shift a phaseless diffraction image is sampled by a detector.
- The measurements are modeled as STFT magnitude measurements:

$$b_{k,j} := \left| \int_{-\infty}^{\infty} f(t) g(t - l_k) e^{-2\pi i \omega_j t} dt \right|^2, \quad 1 \leq k \leq K, \quad 1 \leq j \leq N. \quad (1)$$

- We aim to approximate f (up to a global phase) using these $b_{k,j}$ measurements.

- Given stacked spectrogram samples from (1),

$$\vec{b} = \left(b_{1,1}, \dots, b_{1,N}, b_{2,1}, \dots, b_{K,N} \right)^T \in [0, \infty)^{NK}, \quad (2)$$

approximately recover a piecewise smooth and compactly supported function $f : \mathbb{R} \rightarrow \mathbb{C}$ up to a global phase.

- WLOG assume that the support of f is contained in $[-1, 1]$.
- Motivated by ptychography, we primarily consider the beam function g to also be (effectively) compactly supported within $[-a, a] \subsetneq [-1, 1]$.
- Assume also that g is smooth enough that its Fourier transform decays relatively rapidly in frequency space compared to \hat{f} . Examples of such g include both Gaussians, as well as compactly supported C^∞ bump functions [6].

- Using techniques from [4, 3] on discrete PR adapted to continuous PR, recover samples of \hat{f} at frequencies in $\Omega = \{\omega_1, \dots, \omega_N\}$, giving $\vec{f} \in \mathbb{C}^N$ with $f_j = \hat{f}(\omega_j)$:
 - ▶ First, a truncated lifted linear system is inverted in order to learn a portion of the rank-one matrix $\vec{f}\vec{f}^*$.
 - ▶ Then, angular synchronization is used to recover \vec{f} from the portion of $\vec{f}\vec{f}^*$ above.
- Reconstruct \hat{f} via standard sampling theorems.
- Invert this approximation in order to learn f .
- This linear system is banded and Toeplitz, with band size determined by the decay of \hat{g} : if g is effectively bandlimited to $[-\delta, \delta]$ the computational cost is $\mathcal{O}(\delta N(\log N + \delta^2))$ - **essentially FFT-time** in N for small δ .

Lifted Formulation

Lemma (Lifting Lemma)

Suppose $f : \mathbb{R} \rightarrow \mathbb{C}$ is piecewise smooth and compactly supported in $[-1, 1]$. Let $g \in L^2([-a, a])$ be supported in $[-a, a] \subset [-1, 1]$ for some $a < 1$, with $\|g\|_{L^2} = 1$. Then for all $\omega \in \mathbb{R}$,

$$|\mathcal{F}[f \cdot S_l g](\omega)| = \frac{1}{2} \left| \sum_{m \in \mathbb{Z}} e^{-\pi i l m} \hat{f}\left(\frac{m}{2}\right) \hat{g}\left(\frac{m}{2} - \omega\right) \right|$$

for all shifts $l \in [a - 1, 1 - a]$.

Proof.

- Plancherel's Theorem implies that

$$|\mathcal{F}[f \cdot S_l g](\omega)|^2 = \left| \int_{-\infty}^{\infty} \hat{f}(\omega - \eta) \hat{g}(-\eta) e^{-2\pi i l \eta} d\eta \right|^2.$$

- Applying Shannon's Sampling theorem to \hat{f} and recalling that $\mathcal{F}[f \star g] = \hat{f} \hat{g}$ yield

$$\begin{aligned} |\mathcal{F}[f \cdot S_l g](\omega)|^2 &= \left| \sum_{m \in \mathbb{Z}} \hat{f}\left(\frac{m}{2}\right) \left[\hat{g}(\cdot) e^{-2\pi i l (\cdot)} \star \text{sinc} \pi(m + 2(\cdot)) \right](-\omega) \right|^2 \\ &= \frac{1}{4} \left| \sum_{m \in \mathbb{Z}} \hat{f}\left(\frac{m}{2}\right) e^{-\pi i l (m - 2\omega)} \int_{-l-1}^{-l+1} g(u) e^{-2\pi i u (\frac{m}{2} - \omega)} du \right|^2. \end{aligned}$$

- The result follows by noting the support of g and the Fourier type integral in the last equality.



Lifted Form

We write our measurements in a lifted form

$$|\mathcal{F}[f \cdot S_l g](\omega)|^2 \approx \frac{1}{4} \vec{X}_l^* \vec{Y}_\omega \vec{Y}_\omega^* \vec{X}_l$$

where $\vec{X}_l \in \mathbb{C}^{4\delta+1}$ and $\vec{Y}_\omega \in \mathbb{C}^{4\delta+1}$ are the vectors

$$\vec{X}_l = \begin{pmatrix} e^{\pi i l (2\delta)} \hat{g}(-\delta) \\ e^{\pi i l (2\delta-1)} \hat{g}\left(\frac{1}{2} - \delta\right) \\ \vdots \\ e^{\pi i l \cdot 0} \hat{g}(0) \\ \vdots \\ e^{\pi i l (1-2\delta)} \hat{g}\left(\delta - \frac{1}{2}\right) \\ e^{\pi i l (-2\delta)} \hat{g}(\delta) \end{pmatrix}, \vec{Y}_\omega = \begin{pmatrix} \overline{\hat{f}(\omega - \delta)} \\ \hat{f}\left(\omega - \delta + \frac{1}{2}\right) \\ \vdots \\ \hat{f}(\omega) \\ \vdots \\ \overline{\hat{f}\left(\omega + \delta - \frac{1}{2}\right)} \\ \hat{f}(\omega + \delta) \end{pmatrix}.$$

Lifted Form

We write our measurements in a lifted form

$$|\mathcal{F}[f \cdot \text{Sig}](\omega)|^2 \approx \frac{1}{4} \vec{X}_l^* \vec{Y}_\omega \vec{Y}_\omega^* \vec{X}_l$$

Here, $\vec{Y}_\omega \vec{Y}_\omega^*$ is the rank-one matrix

$$\begin{bmatrix} |\hat{f}(\omega - \delta)|^2 & \cdots & \overline{\hat{f}(\omega - \delta)} \hat{f}(\omega) & \cdots & \overline{\hat{f}(\omega - \delta)} \hat{f}(\omega + \delta) \\ \vdots & \ddots & \vdots & \vdots & \vdots \\ \overline{\hat{f}(\omega)} \hat{f}(\omega - \delta) & \cdots & |\hat{f}(\omega)|^2 & \cdots & \overline{\hat{f}(\omega)} \hat{f}(\omega + \delta) \\ \vdots & \vdots & \vdots & \ddots & \vdots \\ \overline{\hat{f}(\omega + \delta)} \hat{f}(\omega - \delta) & \cdots & \overline{\hat{f}(\omega + \delta)} \hat{f}(\omega) & \cdots & |\hat{f}(\omega + \delta)|^2 \end{bmatrix}.$$

Note the occurrence of the magnitudes of \hat{f} on the diagonal, and the relative phase terms elsewhere.

- Let $\mathbf{F} \in \mathbb{C}^{N \times N}$ be defined as

$$\mathbf{F}_{i,j} = \begin{cases} \overline{\hat{f}\left(\frac{i-2n-1}{2}\right)} \hat{f}\left(\frac{j-2n-1}{2}\right), & \text{if } |i-j| \leq 2\delta, \\ 0, & \text{otherwise,} \end{cases}, \text{ where } n = \frac{N-1}{4}.$$

- \mathbf{F} is composed of overlapping segments of matrices $\vec{Y}_\omega \vec{Y}_\omega^*$ for $\omega \in \{-n, \dots, n\}$.
- Thus, our spectrogram measurements can be written as

$$\vec{b} \approx \text{diag}(\mathbf{G}\mathbf{F}\mathbf{G}^*), \quad (3)$$

where $\mathbf{G} \in \mathbb{C}^{NK \times N}$ is a block Toeplitz matrix encoding the \vec{X}_l 's.

- We consistently vectorize (3) to obtain a linear system which can be inverted to learn \vec{F} , a vectorized version of \mathbf{F} .

- In particular, we have

$$\vec{b} \approx \mathbf{M}\vec{F}, \quad (4)$$

where $\mathbf{M} \in \mathbb{C}^{NK \times N^2}$ is computed by passing the canonical basis of $\mathbb{C}^{N \times N}$ through (3).

- We solve the linear system (4) as a least squares problem.
- Experiments have shown that \mathbf{M} is of rank NK .
- The process of recovering the Fourier samples of f from \vec{F} is known as angular synchronization.

Angular Synchronization

- Angular synchronization is the process recovering d angles $\phi_1, \phi_2, \dots, \phi_d \in [0, 2\pi)$ given noisy and possibly incomplete difference measurements of the form

$$\phi_{ij} := \phi_i - \phi_j, \quad (i, j) \in \{1, 2, \dots, d\} \times \{1, 2, \dots, d\}.$$

- We are interested in angular synchronization problems that arise when performing **phase retrieval** from **local correlation measurements** [4, 3].

Leading Eigenvector \leftrightarrow Phase Vector for $\delta = 1/2$

$$\left[\begin{array}{cccc} |\vec{f}_1|^2 & \vec{f}_1 \vec{f}_2^* & \vec{f}_2 \vec{f}_1^* & |\vec{f}_2|^2 \\ \vec{f}_2 \vec{f}_1^* & |\vec{f}_2|^2 & \vec{f}_2 \vec{f}_3^* & \vec{f}_3 \vec{f}_2^* \\ 0 & \vec{f}_3 \vec{f}_2^* & |\vec{f}_3|^2 & \vec{f}_3 \vec{f}_4^* \\ 0 & 0 & \vec{f}_4 \vec{f}_3^* & |\vec{f}_4|^2 \end{array} \right]^T$$

\downarrow (re-arrange)

$$\left[\begin{array}{cccc} |\vec{f}_1|^2 & \vec{f}_1 \vec{f}_2^* & 0 & 0 \\ \vec{f}_2 \vec{f}_1^* & |\vec{f}_2|^2 & \vec{f}_2 \vec{f}_3^* & 0 \\ 0 & \vec{f}_3 \vec{f}_2^* & |\vec{f}_3|^2 & \vec{f}_3 \vec{f}_4^* \\ 0 & 0 & \vec{f}_4 \vec{f}_3^* & |\vec{f}_4|^2 \end{array} \right] \quad (\mathbb{F}, 4\delta + 1 \text{ entries in band})$$

\downarrow (normalize entrywise)

$$\left[\begin{array}{cccc} 1 & e^{i(\phi_1 - \phi_2)} & 0 & 0 \\ e^{i(\phi_2 - \phi_1)} & 1 & e^{i(\phi_2 - \phi_3)} & 0 \\ 0 & e^{i(\phi_3 - \phi_2)} & 1 & e^{i(\phi_3 - \phi_4)} \\ 0 & 0 & e^{i(\phi_4 - \phi_3)} & 1 \end{array} \right]$$

\downarrow (top eigenvector)

$$\approx [e^{i\phi_1} \ e^{i\phi_2} \ e^{i\phi_3} \ e^{i\phi_4}]^T$$

(Reconstruction of \hat{f} samples) $\left[|\vec{f}_1| e^{i\phi_1} \quad |\vec{f}_2| e^{i\phi_2} \quad |\vec{f}_3| e^{i\phi_3} \quad |\vec{f}_4| e^{i\phi_4} \right]^T$

Leading Eigenvector \leftrightarrow Phase Vector for $\delta = 1/2$

$$\left[\begin{array}{cccc} |\vec{f}_1|^2 & \vec{f}_1 \vec{f}_2^* & \vec{f}_2 \vec{f}_1^* & |\vec{f}_2|^2 \\ \vec{f}_2 \vec{f}_1^* & |\vec{f}_2|^2 & \vec{f}_2 \vec{f}_3^* & \vec{f}_3 \vec{f}_2^* \\ 0 & \vec{f}_3 \vec{f}_2^* & |\vec{f}_3|^2 & \vec{f}_3 \vec{f}_4^* \\ 0 & 0 & \vec{f}_4 \vec{f}_3^* & |\vec{f}_4|^2 \end{array} \right]^T$$

\downarrow (re-arrange)

$$\left[\begin{array}{cccc} |\vec{f}_1|^2 & \vec{f}_1 \vec{f}_2^* & 0 & 0 \\ \vec{f}_2 \vec{f}_1^* & |\vec{f}_2|^2 & \vec{f}_2 \vec{f}_3^* & 0 \\ 0 & \vec{f}_3 \vec{f}_2^* & |\vec{f}_3|^2 & \vec{f}_3 \vec{f}_4^* \\ 0 & 0 & \vec{f}_4 \vec{f}_3^* & |\vec{f}_4|^2 \end{array} \right] \quad (\mathbf{F}, 4\delta + 1 \text{ entries in band})$$

\downarrow (normalize entrywise)

$$\left[\begin{array}{cccc} 1 & e^{i(\phi_1 - \phi_2)} & 0 & 0 \\ e^{i(\phi_2 - \phi_1)} & 1 & e^{i(\phi_2 - \phi_3)} & 0 \\ 0 & e^{i(\phi_3 - \phi_2)} & 1 & e^{i(\phi_3 - \phi_4)} \\ 0 & 0 & e^{i(\phi_4 - \phi_3)} & 1 \end{array} \right]$$

\downarrow (top eigenvector)

$$\approx [e^{i\phi_1} \ e^{i\phi_2} \ e^{i\phi_3} \ e^{i\phi_4}]^T$$

(Reconstruction of \hat{f} samples) $\left[|\vec{f}_1| e^{i\phi_1} \quad |\vec{f}_2| e^{i\phi_2} \quad |\vec{f}_3| e^{i\phi_3} \quad |\vec{f}_4| e^{i\phi_4} \right]^T$

Leading Eigenvector \leftrightarrow Phase Vector for $\delta = 1/2$

$$\left[\begin{array}{cccc} |\vec{f}_1|^2 & \vec{f}_1 \vec{f}_2^* & \vec{f}_2 \vec{f}_1^* & |\vec{f}_2|^2 \\ \vec{f}_2 \vec{f}_1^* & |\vec{f}_2|^2 & \vec{f}_2 \vec{f}_3^* & \vec{f}_3 \vec{f}_2^* \\ 0 & \vec{f}_3 \vec{f}_2^* & |\vec{f}_3|^2 & \vec{f}_3 \vec{f}_4^* \\ 0 & 0 & \vec{f}_4 \vec{f}_3^* & |\vec{f}_4|^2 \end{array} \right]^T$$

\downarrow (re-arrange)

$$\left[\begin{array}{cccc} |\vec{f}_1|^2 & \vec{f}_1 \vec{f}_2^* & 0 & 0 \\ \vec{f}_2 \vec{f}_1^* & |\vec{f}_2|^2 & \vec{f}_2 \vec{f}_3^* & 0 \\ 0 & \vec{f}_3 \vec{f}_2^* & |\vec{f}_3|^2 & \vec{f}_3 \vec{f}_4^* \\ 0 & 0 & \vec{f}_4 \vec{f}_3^* & |\vec{f}_4|^2 \end{array} \right] \quad (\mathbf{F}, 4\delta + 1 \text{ entries in band})$$

\downarrow (normalize entrywise)

$$\left[\begin{array}{cccc} 1 & e^{i(\phi_1 - \phi_2)} & 0 & 0 \\ e^{i(\phi_2 - \phi_1)} & 1 & e^{i(\phi_2 - \phi_3)} & 0 \\ 0 & e^{i(\phi_3 - \phi_2)} & 1 & e^{i(\phi_3 - \phi_4)} \\ 0 & 0 & e^{i(\phi_4 - \phi_3)} & 1 \end{array} \right]$$

\downarrow (top eigenvector)

$$\approx [e^{i\phi_1} \ e^{i\phi_2} \ e^{i\phi_3} \ e^{i\phi_4}]^T$$

(Reconstruction of \hat{f} samples) $\left[|\vec{f}_1| e^{i\phi_1} \quad |\vec{f}_2| e^{i\phi_2} \quad |\vec{f}_3| e^{i\phi_3} \quad |\vec{f}_4| e^{i\phi_4} \right]^T$

Leading Eigenvector \leftrightarrow Phase Vector for $\delta = 1/2$

$$\left[\begin{array}{cccc} |\vec{f}_1|^2 & \vec{f}_1 \vec{f}_2^* & \vec{f}_2 \vec{f}_1^* & |\vec{f}_2|^2 \\ \vec{f}_2 \vec{f}_1^* & |\vec{f}_2|^2 & \vec{f}_2 \vec{f}_3^* & \vec{f}_3 \vec{f}_2^* \\ 0 & \vec{f}_3 \vec{f}_2^* & |\vec{f}_3|^2 & \vec{f}_3 \vec{f}_4^* \\ 0 & 0 & \vec{f}_4 \vec{f}_3^* & |\vec{f}_4|^2 \end{array} \right]^T$$

\downarrow (re-arrange)

$$\left[\begin{array}{cccc} |\vec{f}_1|^2 & \vec{f}_1 \vec{f}_2^* & 0 & 0 \\ \vec{f}_2 \vec{f}_1^* & |\vec{f}_2|^2 & \vec{f}_2 \vec{f}_3^* & 0 \\ 0 & \vec{f}_3 \vec{f}_2^* & |\vec{f}_3|^2 & \vec{f}_3 \vec{f}_4^* \\ 0 & 0 & \vec{f}_4 \vec{f}_3^* & |\vec{f}_4|^2 \end{array} \right] \quad (\mathbf{F}, 4\delta + 1 \text{ entries in band})$$

\downarrow (normalize entrywise)

$$\left[\begin{array}{cccc} 1 & e^{i(\phi_1 - \phi_2)} & 0 & 0 \\ e^{i(\phi_2 - \phi_1)} & 1 & e^{i(\phi_2 - \phi_3)} & 0 \\ 0 & e^{i(\phi_3 - \phi_2)} & 1 & e^{i(\phi_3 - \phi_4)} \\ 0 & 0 & e^{i(\phi_4 - \phi_3)} & 1 \end{array} \right]$$

\downarrow (top eigenvector)

$$\approx [e^{i\phi_1} \ e^{i\phi_2} \ e^{i\phi_3} \ e^{i\phi_4}]^T$$

(Reconstruction of \hat{f} samples) $\left[|\vec{f}_1| e^{i\phi_1} \quad |\vec{f}_2| e^{i\phi_2} \quad |\vec{f}_3| e^{i\phi_3} \quad |\vec{f}_4| e^{i\phi_4} \right]^T$

Leading Eigenvector \leftrightarrow Phase Vector for $\delta = 1/2$

$$\left[\begin{array}{cccc} |\vec{f}_1|^2 & \vec{f}_1 \vec{f}_2^* & \vec{f}_2 \vec{f}_1^* & |\vec{f}_2|^2 \\ \vec{f}_2 \vec{f}_1^* & |\vec{f}_2|^2 & \vec{f}_2 \vec{f}_3^* & \vec{f}_3 \vec{f}_2^* \\ 0 & \vec{f}_3 \vec{f}_2^* & |\vec{f}_3|^2 & \vec{f}_3 \vec{f}_4^* \\ 0 & 0 & \vec{f}_4 \vec{f}_3^* & |\vec{f}_4|^2 \end{array} \right]^T$$

\downarrow (re-arrange)

$$\left[\begin{array}{cccc} |\vec{f}_1|^2 & \vec{f}_1 \vec{f}_2^* & 0 & 0 \\ \vec{f}_2 \vec{f}_1^* & |\vec{f}_2|^2 & \vec{f}_2 \vec{f}_3^* & 0 \\ 0 & \vec{f}_3 \vec{f}_2^* & |\vec{f}_3|^2 & \vec{f}_3 \vec{f}_4^* \\ 0 & 0 & \vec{f}_4 \vec{f}_3^* & |\vec{f}_4|^2 \end{array} \right] \quad (\mathbf{F}, 4\delta + 1 \text{ entries in band})$$

\downarrow (normalize entrywise)

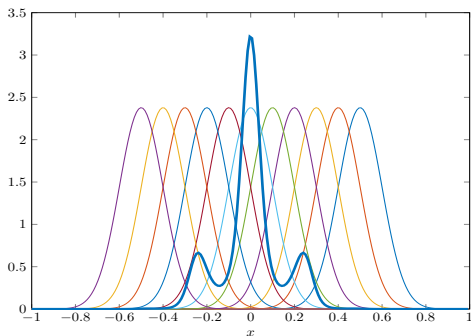
$$\left[\begin{array}{cccc} 1 & e^{i(\phi_1 - \phi_2)} & 0 & 0 \\ e^{i(\phi_2 - \phi_1)} & 1 & e^{i(\phi_2 - \phi_3)} & 0 \\ 0 & e^{i(\phi_3 - \phi_2)} & 1 & e^{i(\phi_3 - \phi_4)} \\ 0 & 0 & e^{i(\phi_4 - \phi_3)} & 1 \end{array} \right]$$

\downarrow (top eigenvector)

$$\approx [e^{i\phi_1} \quad e^{i\phi_2} \quad e^{i\phi_3} \quad e^{i\phi_4}]^T$$

(Reconstruction of \hat{f} samples) $\left[|\vec{f}_1| e^{i\phi_1} \quad |\vec{f}_2| e^{i\phi_2} \quad |\vec{f}_3| e^{i\phi_3} \quad |\vec{f}_4| e^{i\phi_4} \right]^T$

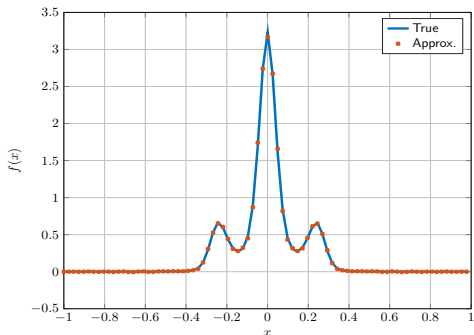
- Consider the Oscillatory Gaussian $f(x) = 2^{\frac{1}{4}} e^{-8\pi x^2} \cos(24x) \chi_{[-1,1]}$.
- Take as window the Gaussian $g(x) = c \cdot e^{-16\pi x^2} \chi_{[-\frac{1}{2}, \frac{1}{2}]}$.



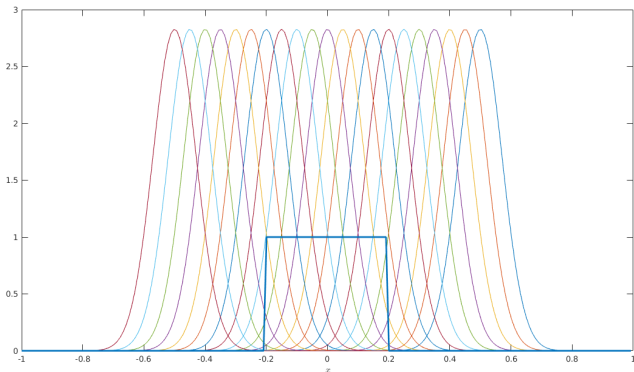
- We use a total of 11 shifts of g , and choose 61 values of ω from $[-15, 15]$ sampled in half-steps, and set $\delta = 7$.

The reconstruction in physical space is shown at selected grid points in the figure below.

The relative ℓ^2 error in physical space is 1.872×10^{-2} .



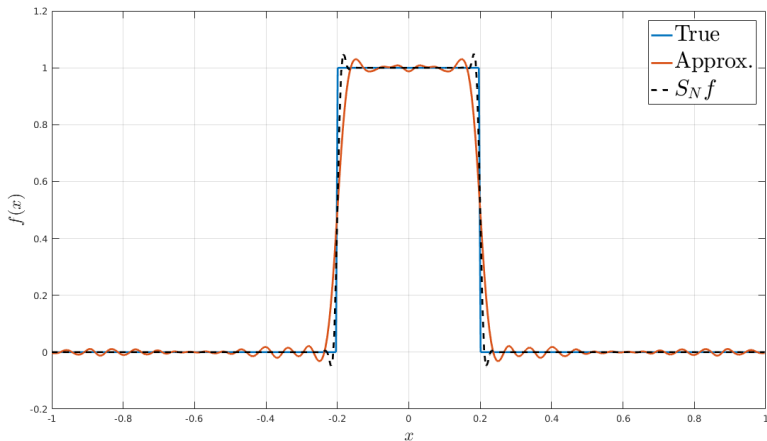
- Consider the Characteristic Function $f(x) = \chi_{[-\frac{1}{5}, \frac{1}{5}]}$.
- Take as window the Gaussian $g(x) = c \cdot e^{-32\pi x^2} \chi_{[-\frac{1}{2}, \frac{1}{2}]}$.



- We use a total of 21 shifts of g , and choose 293 values of ω from $[-73, 73]$ sampled in half-steps, and set $\delta = 10$.

The reconstruction in physical space is shown in the figure below.

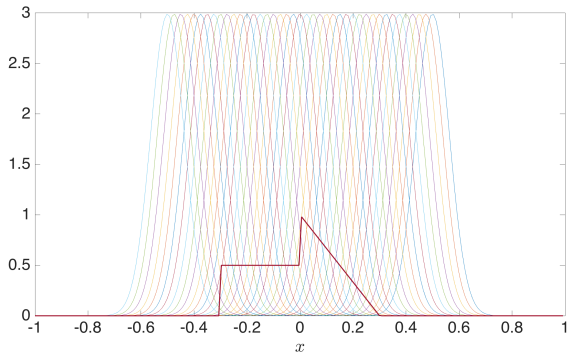
The relative ℓ^2 error in physical space is 1.509×10^{-1} .



- Consider the Piecewise Smooth Function

$$f(x) = \frac{1}{2}\chi_{[-\frac{3}{20}, 0]} + \left(\frac{-10}{3}x + 1\right)\chi_{[0, \frac{3}{20}]}.$$

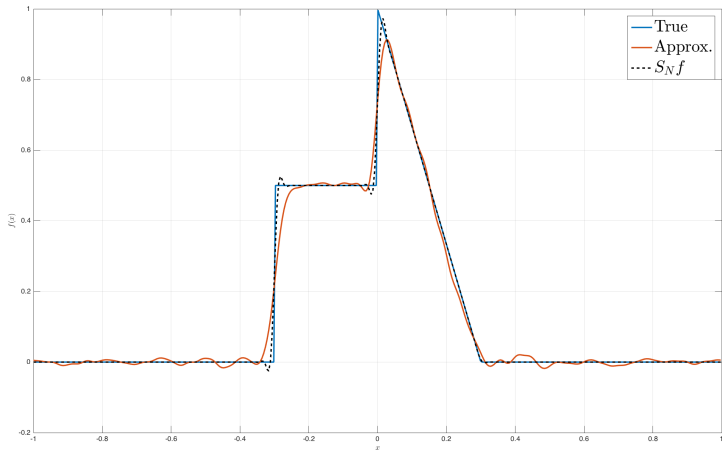
- Take as window the Gaussian $g(x) = c \cdot e^{-32\pi x^2/5}\chi_{[-\frac{1}{2}, \frac{1}{2}]}$.



- We use a total of 41 shifts of g , and choose 281 values of ω from $[-70, 70]$ sampled in half-steps, and set $\delta = 10$.

The reconstruction in physical space is shown in the figure below.

The relative ℓ^2 error in physical space is 1.162×10^{-1} .



References I

- [1] T. Bendory and Y. C. Eldar. Non-convex phase retrieval from STFT measurements. 2016. preprint, arXiv:1607.08218.
- [2] Y. C. Eldar, P. Sidorenko, D. G. Mixon, S. Barel, and O. Cohen. Sparse phase retrieval from short-time Fourier measurements. *IEEE Signal Process. Lett.*, 22(5):638–642, 2015.
- [3] M. A. Iwen, B. Preskitt, R. Saab, and A. Viswanathan. Phase retrieval from local measurements: Improved robustness via eigenvector-based angular synchronization. 2016. preprint, arXiv:1612.01182.
- [4] M. A. Iwen, A. Viswanathan, and Y. Wang. Fast phase retrieval from local correlation measurements. *SIAM J. Imaging Sci.*, 9(4):1655–1688, 2016.
- [5] K. Jaganathan, Y. C. Eldar, and B. Hassibi. STFT phase retrieval: Uniqueness guarantees and recovery algorithms. *IEEE J. Sel. Topics Signal Process.*, 10(4):770–781, 2016.

References II

- [6] S. G. Johnson. Saddle-point integration of C^∞ “bump” functions. 2015. preprint, arXiv:1508.04376.
- [7] S. Marchesini, Y.-C. Tu, and H.-t. Wu. Alternating projection, ptychographic imaging and phase synchronization. *Appl. Comput. Harmon. Anal.*, 41(3):815–851, 2016.
- [8] S. Nawab, T. Quatieri, and J. Lim. Signal reconstruction from short-time Fourier transform magnitude. *IEEE Trans. Acoust., Speech, Signal Process.*, 31(4):986–998, 1983.
- [9] G. E. Pfander and P. Salanevich. Robust phase retrieval algorithm for time–frequency structured measurements. 2016. preprint, arXiv:1611.02540.
- [10] J. Rodenburg, A. Hurst, and A. Cullis. Transmission microscopy without lenses for objects of unlimited size. *Ultramicroscopy*, 107(2):227–231, 2007.

References III

- [11] P. Salanevich and G. E. Pfander. Polarization based phase retrieval for time-frequency structured measurements. In *Proc. 2015 Int. Conf. Sampling Theory and Applications (SampTA)*, pages 187–191, 2015.
- [12] N. Sturmel and L. Daudet. Signal reconstruction from STFT magnitude: A state of the art. In *Int. Conf. Digital Audio Effects (DAFx)*, pages 375–386, 2011.